Mixer, a Homeobox Gene Required for Endoderm Development

Gilbert L. Henry and Douglas A. Melton*

An expression cloning strategy in *Xenopus laevis* was used to isolate a homeobox-containing gene, *Mixer*, that can cause embryonic cells to form endoderm. *Mixer* transcripts are found specifically in the prospective endoderm of gastrula, which coincides with the time and place that endodermal cells become histologically distinct and irreversibly determined. Loss-of-function studies with a dominant inhibitory mutant demonstrate that *Mixer* activity is required for endoderm development. In particular, the expression of *Sox17*α and *Sox17*β, two previously identified endodermal determinants, require *Mixer* function. Together, these data suggest that *Mixer* is an embryonic transcription factor involved in specifying the endodermal germ layer.

Specification of vertebrate germ layers has been extensively studied in recent years and considerable progress has been made in understanding genes and signaling pathways involved in formation of the mesoderm, ectoderm, and the embryonic nervous system (*1*). For example, the *Brachyury* transcription factor is a key regulator of embryonic mesodermal cell specification and, for the most part, the signals inducing neural and epidermal tissues have been identified (*2*). In contrast, relatively little is known about genes that are required to make endoderm in vertebrates. Understanding the embryological specification of the endoderm is a first step toward explaining the organogenesis of all endodermal derivatives, including the thymus, liver, pancreas, intestine, and respiratory tract.

Xenopus endoderm derives from the yolk-rich vegetal region of the blastula. Before gastrulation, these vegetal cells are not irreversibly determined or committed to form endoderm and will differentiate as ectodermal or mesodermal tissues when transplanted into the blastocoel of a host (*3*). Moreover, prospective endodermal cells can be converted to mesodermal and ectodermal cell types by expression of dominant-negative constructs that block transforming growth factor-β (TGF-β) signals (*4*). As gastrulation proceeds, the labile nature of prospective endoderm is lost and the fate of the endoderm becomes restricted to cells that will line the gut tube (*3*).

Differentiation of the numerous endodermal derivatives along the respiratory and gastrointestinal tracts normally occurs in close association with adjacent mesoderm (*5*), but prospective endoderm can undergo some differentiation in the absence of mesoderm, as evidenced by the fact that, when cultured in isolation, vegetal explants from *Xenopus* blastula express endoderm-specific molecular markers (*6*). In this case, expression of these markers reveals a prepattern in the blastula prospective endoderm: anterior vegetal cells autonomously express a pancreas-specific transcription factor, whereas posterior vegetal cells express a small intestine–specific transcript (*4*).

The ability of blastula stage vegetal cells to differentiate in isolation suggests that key regulatory genes are expressed in prospective endoderm. Following this assumption, we constructed a cDNA library from prospective endoderm (blastula to early gastrula vegetal poles) and used a functional screen for endodermal determinants. The objective of the screen was to find genes capable of inducing endoderm in the absence of other complicating germ layers such as the mesoderm. This was accomplished by an expression cloning strategy similar to that used to isolate neuralizing factors and mesoderm inducers (*7*). In this case, pools of prospective endoderm-derived mRNAs were injected into the animal poles of one-cell embryos (*7*) and animal cap explants were removed at the blastula stages and scored 2 days later for expression of endodermal markers in the absence of markers for other germ layers such as mesoderm or neurectoderm (Fig. 1A). Secreted factors such as cerberus, chordin, and Vg1can all induce endoderm in this animal cap assay, but these factors fail the screening test as they also induce either neural or mesodermal cell types.

Woodland and colleagues (*8*) recently identified two transcription factors, *Sox17*α and *Sox17*β, in a subtractive polymerase chain reaction (PCR) screen designed to find genes whose expression is enriched in embryonic endoderm. Both *Sox* genes induce endoderm in animal caps, and endodermal development is blocked in embryos expressing a dominant inhibitory mutant of *Sox17*β. Significantly, the *Sox17* genes are expressed exclusively in the endoderm, which supports the hypothesis that key regulatory factors should be expressed in this germ layer. Here we describe *Mixer* (Mix-like endodermal regulator), a third endoderm-specific factor that, like the *Sox* genes, specifically converts blastula cells to an endodermal

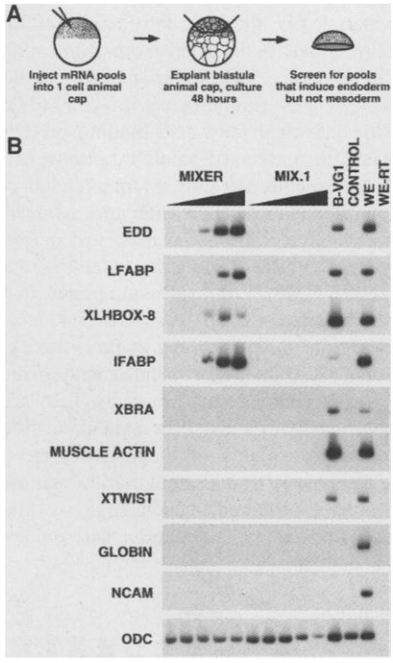

Fig. 1. Expression cloning of *Mixer*, a transcription factor that causes embryonic cells to form endoderm. (**A**) A zygotic endodermal cDNA expression library was screened by injecting pools of mRNAs into the animal hemisphere of one-cell embryos. Pools that specifically induced endodermal, but not mesodermal or neural marker, expression were sib-selected and further reduced to a single clone (29). (**B**) *Mixer* induces endodermal marker expression in the absence of mesodermal and neural differentiation. EDD (9), LFABP (*10*), *XlHbox8* (homologue of *Pdx1*) (*11*), IFABP (*12*) are all endoderm-specific markers. A twofold dilution series ending with 500 pg of mRNA per egg is shown. Unlike *Mixer*, the secreted TGF-β–like factor B-Vg1 induces both mesodermal and endodermal markers (*4*). *Mix.1* does not induce markers of any germ layer in this assay, as demonstrated by a twofold dilution series ending with 500 pg of mRNA (*30*). Higher doses of either *Mix.1* or *Mixer* cause cell death in injected animal caps. The control lane represents uninjected animal caps. All markers were assayed at stage 35 except *Xbra*, which was scored from caps of the same experiment at initiation of gastrulation (stage 10.25). The ubiquitous metabolic factor ornithine decarboxylase (ODC) serves as a loading control and the WE-RT lane is a control of whole embryos assayed by PCR without RT (*31*). The amount of *B-Vg1* mRNA (30 pg) used in this experiment was not sufficient to drive a secondary NCAM induction.

Howard Hughes Medical Institute, Department of Molecular and Cellular Biology, Harvard University, 7 Divinity Avenue, Cambridge, MA 02138, USA.

*To whom correspondence should be addressed. E-mail: dmelton@biohp.harvard.edu

fate (GenBank accession number AF068263). Moreover, through loss-of-function experiments, we show that expression of both *Sox17* genes requires *Mixer* activity.

Using the animal cap endoderm induction assay, we screened 50,000 independent cDNA clones by separating them into 100 pools of 500 clones each. The activity of one clone isolated by this strategy is shown (Fig. 1B). *Mixer* potently induces endoderm as judged by its ability to induce the expression of four markers: endodermin (Edd), a pan-endodermal marker (*9*); the liver fatty acid binding protein (LFABP), an anterior small intestine and liver marker (*10*); *Xlhbox-8*, a pancreatic homeobox gene (homologous to *Pdx1*) (*11*); and the intestinal fatty acid binding protein (IFABP), a marker of small intestine (*12*). With the exception of Edd, all these endodermal markers initiate expression approximately a day after gastrulation ends, just before conversion of the endoderm to epithelium (stages 25 to 30). Edd expression begins just before gastrulation, but it is not endoderm specific until the other three markers are expressed (*9*). Animal caps injected with *Mixer* turn on all endodermal markers that are autonomously expressed in mesoderm-free endodermal explants (*4, 13*). However, a dose response of endodermal marker expression is not observed, which suggests that *Mixer* is a general endodermal determinant that by itself is incapable of generating an anteroposterior pattern (Fig. 1B).

Mixer induces endoderm in the absence of both mesodermal and neural cell types. Brachyury (*Xbra*), a pan-mesodermal marker muscle actin that marks somitic muscle; *Xtwist*, an early ventral-lateral mesodermal marker; globin, a ventral mesodermal marker; and NCAM, a pan-neural marker are all absent in explants expressing *Mixer* (*14*). Like *Mixer*, both *Sox17* genes convert blastula cells specifically to endoderm (*8*). Animal caps induced by the T-box transcription factor *Xbra* express only mesodermal genes (*15*). Thus, *Xbra*, *Mixer*, and the recently described *Sox* genes are unusual in that they are early determinants that specifically cause blastula cells to adopt the fate of a single germ layer.

The 1.4-kb *Mixer* cDNA isolated in the screen is the same size as a single transcript observed in Northern blots (*13*). Analysis of the *Mixer* open reading frame shows that it has high homology to two previously isolated homeobox genes, *Mix.1* and *Mix.2* (*16*). The three genes are 84% identical within the homeobox and 28% identical in the putative transcriptional effector domains. *Mixer* is the least homologous of the three genes: *Mix.1* and *Mix.2* are 70% identical along their entire lengths, whereas *Mix.1* is only 37% identical to *Mixer* (*13*). The *Mix* homeoboxes are most similar to the *Paired* subclass, which have been shown to bind DNA as dimers (*17*).

Because of the sequence similarity between previously identified *Mix* genes and *Mixer*, we tested *Mix.1* in an animal cap assay for endoderm induction. As shown (Fig. 1B), *Mix.1* does not induce endodermal marker expression, consistent with its previously described role in patterning the mesoderm toward a ventral fate (*18*). There are extremely low levels of globin and endodermin expression in animal caps expressing *Mix.1*, but none of the other endodermal markers is appreciably expressed (Fig. 1B).

A time course of expression (Fig. 2A) shows that *Mixer* transcripts are detected for only 6 hours during the gastrula stage. Transcripts for *Mix.1*, *Sox17*α, and *Sox17*β all appear at the midblastula transition (MBT), approximately 3 hours before those of *Mixer*. Both *Mix.1* and *Mixer* transcripts abruptly disappear as gastrulation ends at stage 13. *Sox17*α and -β gene expression continues throughout the neurula and tadpole stages (*8*) (Fig. 2A). Expression of *Mixer* during the gastrula stages coincides with the first point in amphibian development when a trilaminar germ layer arrangement can be histologically discerned. Additionally, it is not until the early gastrula stages that endodermal cells are irreversibly determined toward their eventual fate of lining the gut tube (*3*).

In situ hybridizations on sections of gastrula

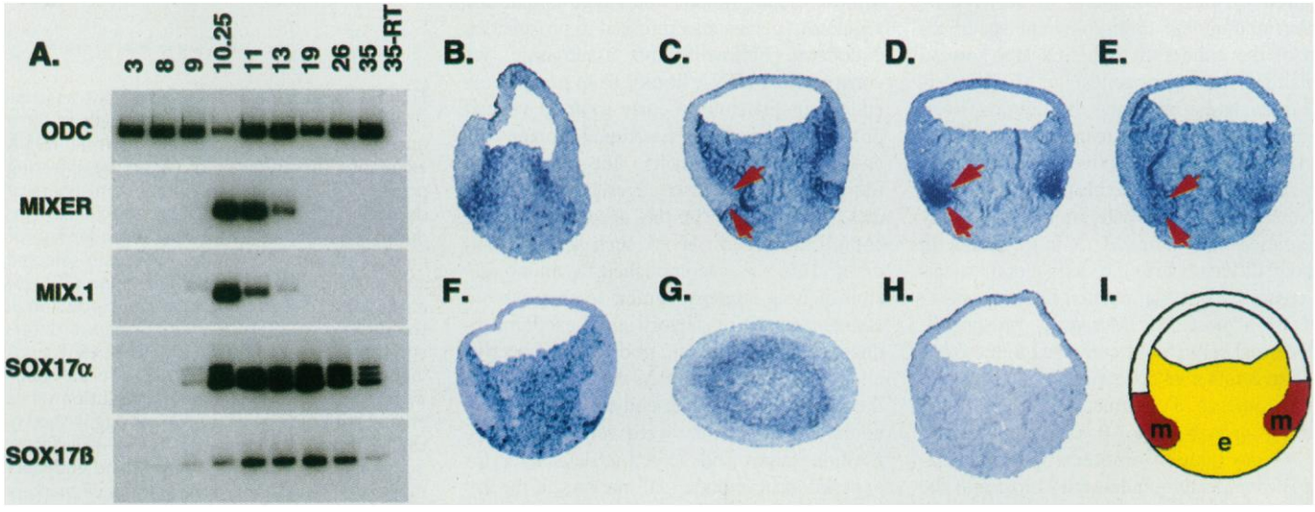

Fig. 2. *Mixer* expression is turned on and off specifically during gastrulation. (**A**) *Mixer* transcripts are detected by RT-PCR at the indicated stages. Expression of *Mix.1* and both *Sox17* genes is observed approximately 3 hours before *Mixer* is detected, but both *Mix.1* and *Mixer* transcripts abruptly disappear with the end of gastrulation at stage 13. The equivalent of one-third of a whole embryo's RNA was used to synthesize cDNA followed by PCR on 1/20th of the synthesized cDNA. ODC serves as a loading control and the 35-RT lane is a control of RT-PCR on stage-35 whole embryo RNA in the absence of RT (*31*). (**B**) Paraffin section of an early gastrula (stage 10.25) embryo hybridized to an antisense *Mixer* probe. Expression is highest at the endodermal edge of the mesendodermal boundary. (**C**) A section from a midgastrula embryo (stage 12) hybridized as in (B). (**D**) A section adjacent to that in (C) hybridized to a probe for the pan-mesodermal marker *Xbra*. Yellow arrows in (C) and (D) highlight the fact that *Xbra* expression is observed where *Mixer* expression is absent. (**E**) Expression of *Mixer* is distinct from that of the closely related gene *Mix.1*. An antisense *Mix.1* probe was hybridized to the section in (E), which is 30 μm away from the sections in (C) and (D). (**F**) A midgastrula section hybridized to a *Sox17*β antisense probe. Expression of *Sox17*β is nearly identical to expression of Mixer at this stage with uniform staining across the endoderm. (**G**) A horizontal section of a midgastrula embryo treated as in (C) displays no strong dorsoventral differences in *Mixer* expression. (**H**) Control of a midgastrula section hybridized to a sense *Mixer* probe. Albino embryos were not used in these in situ experiments and, as a result, a dark rim of pigment is observed across the animal pole of sections shown in (B) to (F) and (H). Arrowheads mark the mesendoderm boundary and are placed in the same position in each panel (*32*). (**I**) Schematic of a midgastrula embryo with endoderm (e) in red and mesoderm (m) in green.

embryos show that *Mixer* transcripts are found specifically in the prospective endoderm (Fig. 2, B, C, and G). Comparing adjacent serial sections that were hybridized with either *Mixer* or *Xbra* antisense probes (Fig. 2, C and D) best shows the endodermal specificity of *Mixer*. *Mixer* expression is strongest at the mesendodermal boundary, which, as gastrulation proceeds, shifts toward the vegetal pole of the embryo (*19*). Consistent with this observation, the edges of the *Mixer* expression domain descend vegetally during gastrulation (Fig. 2, compare B and C). Hybridization to a *Mix.1* probe of a section similar to that in Figure 2D shows expression in both the presumptive endoderm and the marginal zone mesoderm as described (Fig. 2E) (*20*). The gastrula expression of *Sox17*β is shown (Fig. 2F) and it is identical to that observed for *Mixer* except that *Sox17*β expression appears to be more uniform across the interior of the embryo. The *Sox17* genes have identical expression patterns during gastrulation (*8*).

Mixer-induced animal caps are dumbbell shaped with one end more white or yolky in appearance (Fig. 3, A and B). Histological analysis of animal caps coinjected with mRNA encoding the lineage tracer β-galactosidase (βgal) shows that endodermin expression coincides with cells that received *Mixer* mRNA, which are also those that appear yolky or lighter in color in whole explants (Fig. 3, C and D). This suggests that *Mixer* induction of endoderm is cell autonomous, as expected for a determinant that is a transcription factor.

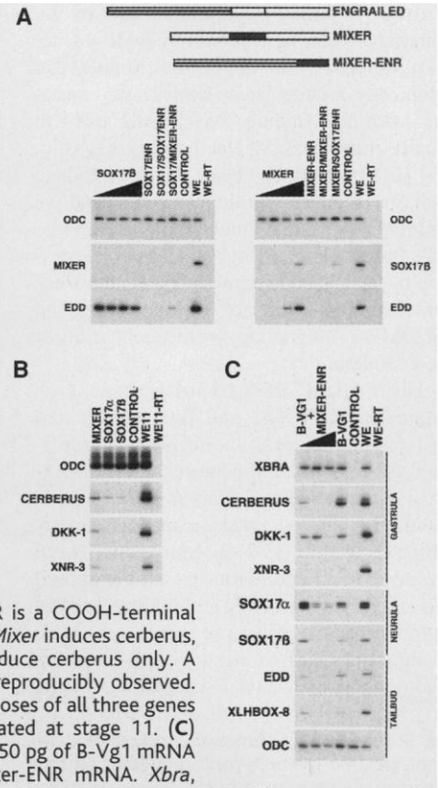

Fig. 4. Structure and activity of Mixer and a dominant inhibitory mutant, Mixer-ENR, made with the engrailed repressor domain. Box diagram shows engrailed repressor domain with a triple bar and Mixer homeobox domain as a black box. The engrailed repressor was fused to the NH_2-terminus of the Mixer homeobox (*28*). Various fusion positions were tested and all behaved similarly. (**A**) *Mixer* induces *Sox17*β in animal cap explants, but *Sox17*β does not induce *Mixer*. A twofold dilution series of *Mixer* and *Sox17*β, from 65 to 500 pg of mRNA injected per egg. Data from the animal caps injected with *Sox17*β and *Mixer* are shown on the left and right, respectively. ODC, *Mixer*, and *Sox17*β data were obtained from stage 11 animal caps, whereas the EDD assays were performed on RNA isolated from stage 35 animal caps. Although both genes induce endoderm (EDD), *Mixer* induces *Sox17* α (data not shown) and *Sox17*β, but neither *Sox17* gene induces *Mixer* (left). For coinjection experiments, the inducer (*Mixer* or *Sox17*β) is injected at 250 pg per egg and the engrailed repressor fusions (Mixer-ENR or Sox17-ENR) are injected at 500 pg per egg. Engrailed repressor fusions alone were at 500 pg of mRNA per egg. Sox17β-ENR is a COOH-terminal fusion to the HMG DNA binding domain (*8*). (**B**) *Mixer* induces cerberus, DKK-1, and Xnr-3, whereas the *Sox17* genes induce cerberus only. A weak induction of Dkk-1 by the *Sox17* genes is reproducibly observed. All RNAs were injected at 500 pg per egg; lower doses of all three genes have the same activity. Animal caps were isolated at stage 11. (**C**) Mixer-ENR blocks the endoderm activity of Vg1; 50 pg of B-Vg1 mRNA was coinjected with 3, 30, or 300 pg of Mixer-ENR mRNA. *Xbra*, cerberus, DKK-1 and *Xnr-3* were assayed at stage 11, stage 19 caps were used to assay expression of both *Sox17* genes, and stage 35 animal caps were used for ODC, EDD, and *Xlhbox-8* assays. ODC for stage 11 and 19 data were similar to those for the stage 35 experiment. ODC serves as a loading control and the WE-RT lane is a control of RT-PCR on stage 11,19, and 35 whole embryo RNA in the absence of RT (*31*).

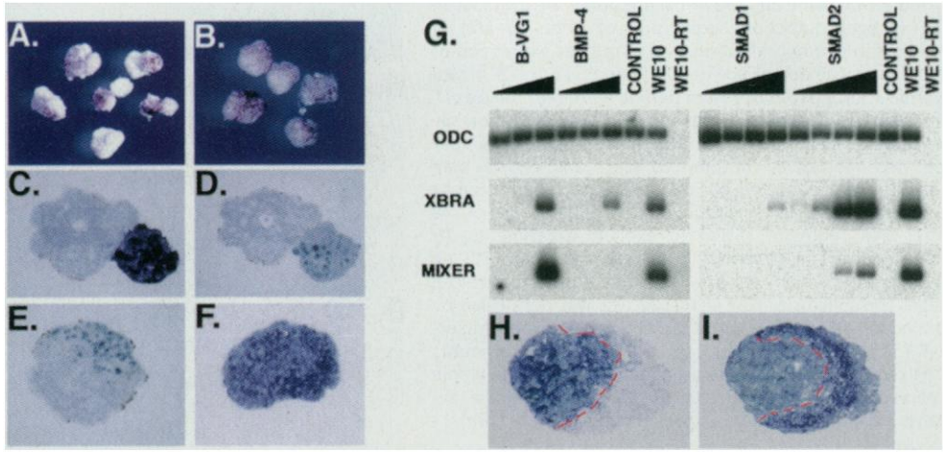

Fig. 3. Induction of endoderm by *Mixer* is cell autonomous and *Mixer* is turned on by Vg1, but not by BMP-4. (**A**) *Mixer*-injected animal caps. (**B**) Uninjected animal caps. Animal caps induced by *Mixer* have a dumbbell shape by the late neurula–early tail bud stages. (**C**) Section from an animal cap coinjected with *Mixer* and βgal mRNAs and hybridized with an antisense endodermin probe (dark blue). (**D**) A section adjacent to that in (C) hybridized with a sense control endodermin probe. In this case, the light blue βgal stain marks the injected cells that coincide with those in (C) expressing endodermin. (**E**) Control of an animal cap injected with βgal mRNA alone and hybridized with an endodermin antisense probe. Light blue stain is for βgal; explants lack the dumbbell shape of the *Mixer*-injected caps shown in (C) and (D). (**F**) Control of a vegetal pole endodermal explant hybridized to an endodermin antisense probe showing ubiquitous expression of this pan-endodermal marker (*32*). (**G**) A 30-fold dilution series of both B-Vg1 (ending at 80 pg of mRNA per egg) and BMP-4 (ending at 2000 pg of mRNA per egg) injected into the animal hemisphere of one-cell embryos, followed by animal cap removal at the blastula stages. Both B-Vg1 and BMP-4 induce *Xbra*, but only B-Vg1 turns on *Mixer* transcription. A similar experiment was done with Smad1 and Smad2 and using a twofold dilution series ending with 500 pg of mRNA per egg (*30*). *Mix.1*, unlike *Mixer*, is induced both by BMP-4 and Vg1 (*18*). ODC is a loading control and the WE10-RT control lane represents a RT-PCR on whole embryo (Stage 10) RNA lacking RT (*31*). (**H**) One animal blastomere of an embryo at the four-cell stage was coinjected with B-Vg1 and βgal mRNAs. Section of an animal cap dissected at the blastula stage, cultured until initiation of gastrulation, and hybridized with a *Mixer* antisense probe. Cells expressing *Mixer* RNA (dark blue) and containing βgal (light blue) overlap in the left two-thirds of the explant. (**I**) A section adjacent to that in (H) was hybridized with an *Xbra* antisense probe. *Xbra* expression (dark blue) is in a crescent of cells adjacent to those expressing *Mixer* and containing the nuclear βgal signal. Red dashes denote the boundary of βgal (injected) cells to the left and uninjected cells to the right expressing *Xbra* (*32*). Explants in (H) to (I) were harvested at stage 10.25 with the remaining explants, (A) to (F), isolated at stage 35.

Mixer is turned on in animal caps by the secreted protein Vg1, but not by BMP-4 (Fig. 3G). Moreover, Smad2, but not Smad1, can ectopically induce *Mixer* expression, consistent with the finding that Smad2 but not Smad1 transduces Vg1/activin signals (Fig. 3G) (*21*). Activin has been shown to induce both *Sox17* genes in animal caps (*8*) and we find that B-Vg1 also induces both genes (Fig. 4C). Induction of *Mixer* and *Sox17* expression by Vg1 is consistent with previous work demonstrating a role for Vg1 signaling, but not BMP-2/4 signaling, in differentiation of the endoderm (*4*).

Histological analysis of animal caps coinjected with Vg1 and βgal shows that Vg1-expressing cells induce *Mixer* expression, whereas distant (uninjected) cells express the mesodermal marker *Xbra* (Fig. 3, H and I). This suggests a mechanism by which a single TGF-β can induce both mesoderm and endoderm in a single animal cap. High levels of Vg1 signaling lead to endodermal specification and lower levels of signaling lead to mesodermal induction (*22*). The endodermal localization of Vg1 transcripts is consistent with such a model (*23*).

Because the expression pattern of the *Sox* genes is essentially identical to that of *Mixer* during the gastrula period and all three genes induce endoderm in animal cap explants, we tested whether one gene might act upstream of the others. *Mixer* induces the expression of both *Sox17* genes in animal cap explants, but neither *Sox17* gene induces *Mixer* (Fig. 4A) (*24*). Further analyses of animal caps in the gastrula stage reveal other differences among these endodermal determinants. *Mixer* induces the expression of cerberus (*25*), *Xenopus* nodal related-3 (*Xnr-3*) (*26*), and *DKK-1* (*27*), whereas *Sox17*α and *Sox17*β induce only cerberus (Fig. 4B). Both cerberus and DKK-1 are expressed in the anterior endoderm of embryos in the gastrula stage and have been implicated in formation and function of the head organizer. *Xnr-3* is also expressed in the gastrula endoderm and has been shown to be a downstream target of the Wnt signaling pathway. The endodermal marker endodermin is induced by *Mixer* and the *Sox17* genes, although the latter do so at lower doses of injected mRNA (Fig. 4A).

A dominant inhibitory mutant of *Mixer* was constructed by fusing the NH_2-terminal transcriptional repressor domain of the *Drosophila* engrailed protein to the homeobox of *Mixer* (Fig. 4A) (*28*). This construct, Mixer-ENR, blocks the ability of *Mixer*, but not *Sox17*β, to induce endoderm in animal cap assays. In a similar experiment, expression of both *Mixer* and *Sox17*β is blocked by a Sox17β engrailed repressor fusion (Fig. 4A). These experiments suggest that *Mixer* is upstream of *Sox17*α and *Sox17*β. However, both *Sox* genes appear 3 hours before *Mixer* in normal development. A plausible explanation for these data is that *Mixer* positively maintains expression of the *Sox17* genes in the endoderm during gastrulation, with all three genes initiating expression independently of one another.

To test whether *Mixer* is required for the maintenance of *Sox17* expression, we analyzed animal caps dissected from embryos coinjected with Mixer-ENR and B-Vg1 RNAs.

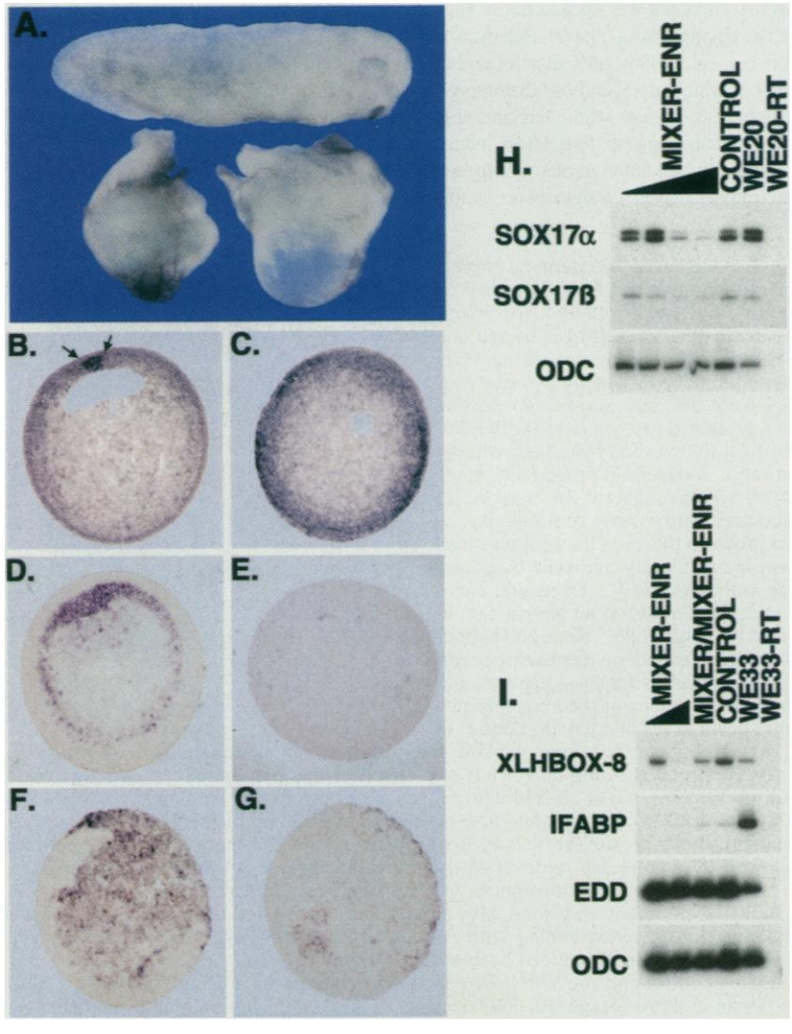

Fig. 5. Loss of *Mixer* function blocks endodermal development. (**A**) Mid-tail bud, control injected embryo (stage 31) is shown above two embryos derived from fertilized eggs injected in the vegetal hemisphere with 150 pg of Mixer-ENR mRNA. Gross morphology of the embryos injected with Mixer-ENR is similar to that observed after injection of a Sox17β-ENR fusion (*8*). (**B**, **D**, and **F**) Transverse sections of control midgastrula (stage 11) embryos for comparison to transverse sections of mid-gastrula (stage 11) embryos injected at the one-cell stage with 500 pg of Mixer-ENR mRNA per egg (**C**, **E**, and **G**). (B and C) In situ hybridization using an *Xbra* antisense probe. Arrowheads in (B) highlight notochord expression of *Xbra*. (D and E) Cerberus in situ hybridization. Note stronger expression of cerberus on the dorsal side in (D). (F and G) *Sox17*β in situ hybridization. (**H**) *Mixer* function is required for *Sox17* expression in endodermal explants. A twofold dilution series of Mixer-ENR mRNA, from 65 to 1000 pg of mRNA per egg, was injected at the one-cell stage and vegetal pole explants were dissected at late blastula and harvested at stage 20. Note that it is possible to use higher levels of the Mixer-ENR repressor fusion in explant experiments. (**I**) Experiment similar to that in (H) except that 30 and 300 pg of Mixer-ENR mRNA per egg was injected at the one-cell stage. The specificity test or rescue test was performed by coinjecting *Mixer* (500 pg of mRNA per egg) and Mixer-ENR (300 pg of mRNA per egg). Although larger amounts of Mixer-ENR mRNA can be used in explants than in whole embryos, it is difficult to culture these vegetal pole explants past the mid-tail bud period (stage 30 or more).

As shown (Fig. 4C), the dominant inhibitory *Mixer* mutant blocked the ability of B-Vg1 to induce late endodermal markers such as EDD and *Xlhbox-8*. In animal caps from the same experiment, isolated at the gastrula stages, DKK-1, cerberus, and *Xnr-3* are all blocked. At stage 9, both *Sox* genes are induced by B-Vg1 in the presence of the Mixer-ENR fusion (data not shown). However, during gastrulation and later at the neurula stages, *Sox17*α and *Sox17*β transcripts are severely reduced (Fig. 4C). Thus, *Sox17* gene expression is not maintained when *Mixer* activity is blocked. Additionally, mesodermal development in animal caps coinjected with B-Vg1 and Mixer-ENR is unaffected, consistent with *Mixer* being an endoderm-specific determinant.

A key test for *Mixer* function is the developmental phenotype of whole embryos expressing the Mixer-ENR fusion. As shown (Fig. 5A), Mixer-ENR–injected embryos are severely affected by the repressor fusion and exhibit anterior truncation and loss of head structures as well as defective gut development; 30% of embryos injected with 150 to 200 pg of mRNA encoding the engrailed repressor fusion develop as shown (Fig. 5A) and the remainder display a similar, but less severe, phenotype with shortening of the anteroposterior axis and defective head formation ($n = 220$). Late endodermal markers are variably expressed in these embryos. Injecting higher doses of Mixer-ENR leads to lethality during gastrulation, presumably because of the complete failure to form the leading anterior (pharyngeal) endoderm.

The block to gastrulation and accompanying lethality led us to examine the *Mixer* loss-of-function phenotype at earlier stages of development. Gastrula stage embryos in which *Mixer* function was blocked were analyzed by in situ hybridization. The expression of *Sox17*β, cerberus, and *Xnr-3* are all strongly reduced in embryos expressing Mixer-ENR mRNA (Fig. 5, D to G). The lack of cerberus expression is consistent with the severe head phenotype (anterior loss) observed in late stage embryos (Fig. 5A). *Brachyury* expression is not reduced by the Mixer-ENR fusion and, in fact, appears to be higher or less concentrated in injected embryos (Fig. 5, B and C). It is possible that this effect on *Brachyury* expression is a result of blocking the activity of other *Mix* transcription factors. Alternatively, this alteration in mesodermal marker expression could reflect defects in cell movements, and we note that late gastrula embryos do not form an embryonic gut lumen or archenteron (Fig. 5, B, and C). These injected embryos initially form a blastopore, but it regresses before stage 13. Similar gastrulation defects are observed in embryos lacking *Sox17* activity (*8*), and together these findings suggest that the endoderm is required for mesodermal cell movements and gastrulation.

We have further assessed the effect of the Mixer-ENR fusion by assaying gene activities in endodermal explants. Vegetal pole explants dissected from embryos injected with Mixer-ENR lack *IFABP* and *Xlhbox-8* expression (Fig. 5I). This block in gene expression is completely rescued by coinjection of wild-type *Mixer* RNA, which suggests that the block is specific. *Mix.1* does not rescue in similar explant assays. Unlike *IFABP* and *Xlhbox-8*, *Edd* expression is not affected by the Mixer-ENR fusion. There are several possible explanations for this finding, one of which is that *Mixer* is involved in development of a subset of endodermal cells. In younger endodermal explants, both *Sox17* genes initiate expression at the MBT, but by the neurula stages they are strongly downregulated in the absence of *Mixer* function (Fig. 5H). Thus, as suggested by the animal cap induction experiments, *Mixer* is required to maintain the expression of both *Sox17* genes in vegetal cells.

In summary, this report provides several lines of evidence to support the conclusion that *Mixer* is a key endodermal determinant. *Mixer* expression drives cells into an endodermal lineage, diverting them from their specification toward ectoderm. In accord with this inducing activity, *Mixer* transcripts are found exclusively in gastrula stage prospective endoderm, a period recognized as the first point at which the endoderm is visible histologically and irreversibly determined (*3*). *Mixer* is required to maintain expression of both *Sox17* genes, themselves previously shown to be required for endodermal development. Finally, loss of *Mixer* function blocks development of the endoderm. Future experiments should aim to determine whether a homologous *Mixer* gene functions to specify endodermal cell lineages in other vertebrates including zebrafish, chickens, and mice.

References and Notes

1. D. S. Kessler and D. A. Melton, *Science* **266**, 596 (1994); P. S. Klein and D. A. Melton, *Endocr. Rev.* **15**, 326 (1994); J. M. W. Slack, *Mech. Dev.* **41**, 91 (1993).
2. A. Hemmati-Brivanlou and D. A. Melton, *Cell* **88**, 13 (1997); Y. Sasai and E. De Robertis, *Dev. Biol.* **182**, 5 (1997); J. C. Smith, *Curr. Opin. Genet. Dev.* **7**, 474 (1997).
3. J. Heasman, C. C. Wylie, P. Hausen, J. C. Smith, *Cell* **37**, 185 (1984); C. C. Wylie, A. Snape, J. Heasman, J. C. Smith, *Dev. Biol.* **119**, 496 (1987).
4. G. L. Henry, I. H. Brivanlou, D. S. Kessler, A. Hemmati-Brivanlou, D. A. Melton, *Development* **122**, 1007 (1996).
5. T. S. Okada, *Mem. Coll. Sci. Univ. Kyoto* **20**, 157 (1953); T. S. Okada, *ibid.* **21**, 1 (1954); T. S. Okada, *ibid.*, p. 7; C. Takata, *Embryologica* **5**, 38 (1960).
6. L. W. Gamer and C. V. E. Wright, *Dev. Biol.* **171**, 240 (1995); (*4*).
7. W. C. Smith and R. M. Harland, *Cell* **67**, 753 (1991); *ibid.* **70**, 829 (1992); J. C. Baker and R. M. Harland, *Genes Dev.* **10**, 1880 (1996).
8. C. Hudson, D. Clements, R. V. Friday, D. Stott, H. R. Woodland, *Cell* **91**, 397 (1997).
9. Y. Sasai, B. Lu, S. Piccolo, E. M. De Robertis, *EMBO J.* **15**, 4547 (1996).
10. Stage 30 *Xenopus* cDNA, synthesized by conventional methods, was subjected to reverse transcription-PCR (RT-PCR) with degenerate primers directed against the following regions, conserved in all known liver isoforms of the fatty acid binding protein: Ile-Gln-Lys-Gly-Lys-Asp-Ile-Lys-Gly and Glu-Gly-Asp-Asn-Lys-Leu-Val-Thr, corresponding to amino acids 29 to 37 and 86 to 93, respectively (GenBank accession number AF068301). In situ hybridizations of stage 35 to 40 embryos reveals expression in the anterior small intestine and liver analogous to expression of rat *LFABP* [J. I. Gordon *et al.*, *J. Biol. Chem.* **258**, 3356 (1983)].
11. C. V. E. Wright, P. Schnegelsberg, E. M. De Robertis, *Development* **105**, 787 (1988).
12. G. L. Henry, I. H. Brivanlou, D. S. Kessler, A. Hemmati-Brivanlou, D. A. Melton, *ibid.* **122**, 1007 (1996); Y. Shi and W. Par Hayes, *Dev. Biol.* **161**, 48 (1994).
13. G. L. Henry and D. A. Melton, unpublished data.
14. J. C. Smith, B. M. J. Price, J. B. A. Green, D. Wiegel, B. G. Herrmann, *Cell* **71**, 731 (1991); F. Stutz and G. Sphor, *J. Mol. Biol.* **187**, 349 (1986); N. D. Hopwood, A. Pluck, J. B. Gurdon, *Cell* **59**, 893 (1989); D. Banville and J. G. Williams, *Nucleic Acids Res.* **13**, 5407 (1985); C. R. Kintner and D. A. Melton, *Development* **99**, 311 (1987).
15. V. Cunliffe and J. C. Smith, *Nature* **358**, 427 (1992).
16. F. M. Rosa, *Cell* **57**, 965 (1989); P. D. Vize, *Dev. Biol.* **177**, 226 (1996).
17. D. Wilson, G. Sheng, T. Lecuit, N. Dostatni, C. Desplan, *Genes Dev.* **7**, 2120 (1993).
18. P. E. Mead, I. H. Brivanlou, C. M. Kelley, L. I. Zon, *Nature* **382**, 357 (1996).
19. D. V. Bauer, S. Huang, S. A. Moody, *Development* **120**, 1179 (1994).
20. F. M. Rosa, *Cell* **57**, 965 (1989).
21. J. M. Graff, A. Bansal, D. A. Melton, *ibid.* **85**, 479 (1996).
22. A. Hemmati-Brivanlou and D. A. Melton, *ibid.* **77**, 273 (1994); D. S. Kessler and D. A. Melton, unpublished observation.
23. D. L. Weeks and D. A. Melton, *Cell* **51**, 861 (1987).
24. Data not shown for *Sox17*α.
25. T. Bouwmeester, S. Kim, Y. Sasai, B. Lu, E. M. De Robertis, *Nature* **382**, 595 (1996).
26. W. C. Smith *et al.*, *Cell* **82**, 37 (1995).
27. A. Glinka *et al.*, *Nature* **391**, 357 (1998).
28. J. B. Jaynes and P. H. O'Farrell, *ibid.* **336**, 744 (1988); F. L. Conlon, S. G. Sedgwick, K. M. Weston, J. C. Smith, *Development* **122**, 2427 (1996).
29. In this study, a cDNA expression library was constructed from stage 9 to 10.25 vegetal pole explants. Poly(A)-enriched RNA was converted to cDNA by the Gibco BRL plasmid cDNA synthesis system. Double-stranded cDNA was then directionally ligated to a modified form of pCS2, which we refer to as pCS300. Briefly, pCS300 differs from pCS2 in that the polylinker II Not I site was moved to the polylinker I area and an Asc I and Pme I site were added to the polylinker II area. This vector is similar in design to pCS100 [J. C. Baker and R. M. Harland (1996)]. Library transformants were divided into pools of 500 clones each by manually scraping LB/ampicillin plates. In vitro transcribed mRNA was then synthesized from Asc I–linearized templates with the Ambion Megascript system. Positive pools were split into 60 pools of 10 clones each and then into 15 pools of 1 clone each. The unamplified expression library contained 530,000 independent clones (*7*).
30. For library screening, 2 to 5 ng of in vitro transcribed capped mRNA was injected into the animal pole of one-cell *Xenopus* embryos in 3% Ficoll containing 0.5× MMR. All other injections were done similarly, as indicated in the figure legends. Explants were reared in 0.5× MMR [50 mM NaCl, 1 mM KCl, 1 mM $CaCl_2$, 0.5 mM $MgCl_2$, 2.5 mM Hepes (pH 7.4)] at 16° to 23°C.
31. RT-PCR was performed as described in (*4*). Primer sets are either described below or referenced (sequences are 5′ to 3′). All explants, including those

used in library construction, were harvested by the Trisolv method. NCAM, GLOBIN, XTWIST, MUSCLE ACTIN, *IFABP* (*4*); *Xlhbox-8* (*9*); *XBRA* [P. A. Wilson and D. A. Melton, *Curr. Biol.* **4**, 676 (1994)]; *EDD*, *ODC* (*25*); *LFABP*, up-ACCGAGATTGAACAGAATGG; down-CCTCCATGTTTACCACGGAC; *MIX.1*, up-CCCAGGCATCATCCAATGTC; down-TGACACGGCTCTTGGTTGGC; *MIXER*, up-CACCAGCCCAGCACTTAACC; down-CAATGTCACATCAACTGAAG; *Sox17α*, *Sox17β* (*8*).

32. In situ hybridization was performed as described in (*4*). Gastrula stage embryos were fixed in paraformaldehyde, cleared in butanol, and mounted in paraffin. All other sectioned material was fixed in MEMFA [0.1 M Mops (pH 7.4), 2 mM EGTA, 1 mM Mg SO_4, 3.7% formaldehyde], cleared in xylene, and mounted in paraffin. All sections are 10 μm thick. For *Mixer* and *Mix.1* in situ hybridization, probes were constructed from sequences 3′ to the homeobox. The *Edd* and *Xbra* in situ probes have been described in [(*9*); J. C. Smith *et al.*, *Cell* **71**, 731 (1991)]. βgal activity was measured according to standard protocols.

33. Supported in part by grants from the National Institutes of Health and the Howard Hughes Medical Institute (HHMI). G.L.H. was supported by a predoctoral grant from the National Science Foundation and D.A.M. is an investigator of the HHMI. We acknowledge the help of R. Harland for advice on expression libraries, K. Symes for histological advice, R. Nicholls and S. Newfield for sequence alignment advice, P. Rahaim and J. Rush of the HHMI Biopolymers facility for both DNA synthesis and sequencing, E. Wu for computing advice, P. Mead for communicating data before publication, H. Woodland and D. Clements for providing *Sox17* clones, and all members of the Melton lab for helpful discussions—in particular L. Chen, Z. Balsara, S. Kim, M. Hebrok, O. Kelley, E. Wu, K. O'Donnel, C-J. Lai, J. Wells, P. Klein, D. Kessler, and C. Dohrman.

28 October 1997; accepted 22 May 1998

Visualization of Specific B and T Lymphocyte Interactions in the Lymph Node

Paul Garside,* Elizabeth Ingulli,* Rebecca R. Merica, Julia G. Johnson, Randolph J. Noelle, Marc K. Jenkins†

Early events in the humoral immune response were visualized in lymph nodes by simultaneous tracking of antigen-specific CD4 T and B cells after immunization. The T cells were initially activated in the T cell areas when the B cells were still randomly dispersed in the B cell–rich follicles. Both populations then migrated to the edges of the follicles and interacted there, resulting in CD154-dependent B cell proliferation and germinal center formation. These results provide visual documentation of cognate T-B cell interactions and localize them to the follicular border.

Antigen-specific T and B lymphocytes are essential for humoral immune responses to many antigens (*1*). It is known that the T cell dependence of antibody production is related to the efficient capture and internalization of antigen by surface immunoglobulin (Ig), which allows antigen-specific B cells to efficiently present antigenic peptide–major histocompatibility complex (MHC) molecules to antigen-specific T cells (*2*). The T cells are thus positioned to provide stimulatory surface molecules and cytokines, thereby helping the B cells produce antibodies (*3*).

It is widely believed that the earliest T-B cell interactions during the primary response occur as a result of the movement of antigen-specific B cells from the B cell–rich follicles into the T cell–rich areas, where they meet antigen-specific T cells (*4*). However, T-B cell interactions have not been directly observed because of technical difficulties related to simultaneous in situ detection of the rare naïve T and B cells specific for a given antigen.

We addressed this problem by tracking small populations of antigen receptor transgenic T and B lymphocytes after adoptive transfer into normal recipients. CD4 T cells from DO11.10 T cell antigen receptor (TCR) transgenic (BALB/c × C57BL/6)F_1 mice (*5*) specific for chicken ovalbumin (cOVA) (amino acid residues 323 to 339) complexed to I-A^d (*6*) and MD4 Ig transgenic (BALB/c × C57BL/6)F_1 mice with B cells specific for hen egg lysozyme (HEL) (*7*) were transferred (*8*) into nontransgenic (BALB/c-Igh^b × C57BL/6)F_1 animals. The DO11.10 CD4 T cells were identified in the lymph nodes of the recipients by flow cytometry after staining with the anticlonotypic TCR monoclonal antibody (mAb) KJ1-26 (*9*); labeled HEL or antibody specific for the IgM^a (anti-HEL Ig) allotype was used to identify MD4 B cells (*10*).

cOVA was chemically coupled to HEL to produce an antigen (cOVA-HEL) containing linked epitopes that could be recognized by both transgenic populations (cOVA-HEL) (*11*). Immunization with cOVA-HEL caused the DO11.10 CD4 T cells in the draining lymph nodes to undergo clonal expansion that was apparent by day 2, was maximal on days 3 and 4, and declined thereafter (Fig. 1A).

MD4 B cell expansion in the lymph nodes was detected 3 days after immunization, peaked on day 4 or 5, and then declined (Fig. 1A). Maximal clonal expansion of the MD4 B cells was dependent on the presence of the DO11.10 T cells, because a much reduced response was observed in mice that received B cells alone (Fig. 1A). The MD4 B cells responded weakly when recipients of DO11.10 T cells and MD4 B cells were immunized with a mixture of cOVA and HEL that had been conjugated to turkey OVA (tOVA-HEL) (Fig. 1B), which lacks the appropriate peptide recognized by the DO11.10 TCR (Fig. 1C). The poor response of the B cells in this situation could not be explained by a failure of T cell activation because the DO11.10 T cells responded well after immunization with cOVA plus tOVA-HEL (Fig. 1C). The simplest explanation for these results is that MD4 B cells were efficiently activated to proliferate in vivo only when expression of anti-HEL Ig allowed efficient uptake of cOVA and presentation of cOVA peptide to DO11.10 T cells.

This conclusion was supported by the finding that blockage of CD154 (CD40 ligand), a surface molecule expressed by activated CD4 T cells that provides a contact-dependent signal to B cells (*12*), completely inhibited clonal expansion (Fig. 1D) and antibody production (*13*) by the MD4 B cells. In contrast, treatment with antibody to CD154 (anti-CD154) inhibited clonal expansion of the DO11.10 T cells by only about 50% (Fig. 1D). These findings suggest that the previously described effects of CD154 blockade on antibody production and germinal center formation (*12*) can be explained by a failure of B cell clonal expansion.

Immunohistochemical analyses were carried out to determine whether the cognate interactions predicted by the functional experiments could be directly observed in situ. After adoptive transfer, but before immunization, the DO11.10 T cells were dispersed throughout the T cell–rich paracortical regions of the lymph node but were not present in the B cell–rich follicles (Fig. 2A). In contrast, the MD4 B cells were localized mainly in follicles (Fig. 2E). One day after immunization, the DO11.10 T cells had not increased

P. Garside, University of Glasgow, Department of Immunology, Western Infirmary, Glasgow, G11 6NT, United Kingdom. E. Ingulli, Department of Pediatrics, University of Minnesota Medical School, Minneapolis, MN 55455, USA. R. R. Merica, J. G. Johnson, M. K. Jenkins, Department of Microbiology and the Center for Immunology at the University of Minneota Medical School, Minneapolis, MN 55455, USA. R. J. Noelle, Dartmouth Medical College, Department of Microbiology, Lebanon, NH, USA.

*These authors contributed equally to this work.
†To whom correspondence should be addressed.